Heat-dependent Loop Melting Drives TRPV1 Opening

Running title: Digit codes in heat-sensing TRPV1

Guangyu Wang*

Department of Physiology and Membrane Biology, University of California School of Medicine, Davis, CA, USA

Department of Drug Research and Development, Institute of Biophysical Medico-chemistry, Reno, NV, USA

* Author to whom correspondence should be addressed; E-mail: gary.wang10@gmail.com

Abstract

Non-covalent crosslinking interactions in bio-macromolecules are individually weak but collectively important. How they take a concerted action in a complex biochemical reaction network to realize their thermal activity and stability is still challenging to study. Here graph theory was used to investigate how the temperature-dependent non-covalent crosslinking interactions as identified in the structures of the thermo-gated capsaicin receptor TRPV1 could form little loops with minimal lengths to control the specific activation threshold and the lipid-dependent temperature sensitivity and the use-dependent desensitization. The results showed that the heat-evoked melting of the biggest little loop may initiate a specific temperature threshold for channel activation while smaller little loops with strong H-bonds may balance between open and inactivated states for heat efficacy and the use-dependent desensitization. Altogether, both the biggest and smaller little loops may be necessary for the lipid-dependent temperature sensitivity. Therefore, this loop thermodynamic model may be broadly significant for thermal stability and activity of supramolecular architectures. (156 words)

Keywords: desensitization; loop thermodynamics; lipid; non-covalent crosslinking interaction; temperature sensitivity; threshold; TRP channel

1. INTRODUCTION

Temperature is important in everyday life. Transient receptor potential (TRP) vanilloid-1 (TRPV1) is well-known as a noxious heat sensor in a primary afferent neuron of the dorsal root and the trigeminal ganglia. Its activation allows sodium or calcium to be permeable to a channel pore. With an activation threshold (~42 °C) above a normal human body temperature 37 °C and a temperature coefficient Q_{10} higher than 20, this channel can work as a bio-thermometer to monitor a noxious heat signal above 42 °C and to regulate the human body temperature. [1-4] In addition to the physical stimuli, capsaicin can also activate TRPV1, producing hot sensation. As cold can decrease the capsaicin-evoked activity of TRPV1, [5] the same gating pathway seems to be shared by both stimuli. On the other hand, residues sensitive to both physical and chemical stimuli are different in TRPV1, suggesting their different gating pathways. [6-9]

TRPV1 is a homotetramer with each monomer consisting of six transmembrane helices. The first four segments (S1–S4) form a voltage-sensor-like domain (VSLD) while the last two (S5 and S6), together with the intervening loop and the pore helix and the extracellular cap-like pore turret between S5 and S6, are folded as a pore domain. The pore domain is surrounded by the VSLD in a domain-swapped arrangement. The cation conductance pathway centers in the pore domain. A hydrophobic constriction around I697 forms a lower S6 gate while the segment from G643 to D646 (^{643}GMGD^{646}) between S5 and S6 (S5-P-S6) in rat TRPV1 (rTRPV1) acts as a short selectivity filter. The S4–S5 linker, which is a short amphipathic helix and almost parallel to the cytoplasmic membrane, couples the VSLD with the pore domain for channel gating. Thus, the overall structure of the TRPV1 channel resembles that of the voltage-gated ion channel. [10-11] However, TRPV1 has a conserved TRP domain, which runs parallel to the inner leaflet of the membrane by virtue of a sharp bend after S6, not only linking the S6 gate crossing bundle but also interacting with the S4–S5 linker and the pre-S1 domain in favor of allosteric coupling between different gating domains. In addition, the characteristic ankyrin repeats within the cytoplasmic N terminus can tether cytoplasmic N- and C-terminal domains for channel assembly. [11-14] Although the structural basis for the chemical stimuli such as capsaicin has been clear, [6, 15-16] the heat-evoked gating pathway is still unknown for TRPV1. The remaining questions include what structural factors control the specific temperature threshold 42 °C, [17] how the phosphatidylinositol (PI) lipid at the capsaicin site increases the temperature sensitivity Q_{10} from

16.4 to 28.2, [14] and what structural factors govern the use-dependent desensitization above 42 °C in an irreversible manner. [1, 8, 18-19]

Since 2013 a DNA hairpin thermal sensor with a limited poly-A loop length has been created to monitor a change in a biological microenvironment. When temperature increases above a threshold in a range from 34 °C to 73 °C, the hydrogen bonds between the bases in the DNA duplex are broken so that the DNA loop melts with a characteristic sigma plot. [20] Generally, when the loop length declines from 20 to 10 A's or the H-bonded G-C base-pairs double from 2 to 4, the temperature threshold can be raised more than 20 degrees. [20] Similarly, TRPV1 can be activated above a specific temperature threshold 42 °C and also with a characteristic sigma plot at elevated temperatures. [17] In this regard, it is fitting to ask if the thermosensitive TRPV1 channel exploits a series of non-covalent crosslinking interactions to form little topological loops with the minimal lengths to control the specific temperature thresholds and the lipid-dependent temperature sensitivity (Q_{10}) and the use-dependent desensitization in an irreversible manner. In this computational study, graph theory was used as a novel tool to examine this hypothesis by analyzing the cryo-electron microscopy (cryo-EM) structural data of rTRPV1 with or without PI-bound at the capsaicin site around the temperature threshold. When the biggest with the relatively longest path among little loops along the gating pathway was identified, a loop thermodynamic model, which was developed from the DNA hairpin, was used to generate several melting temperatures (T_m) which were found comparable to the experimental thresholds (T_{th}). Further, once structural thermo-sensitivity (Ω_{10}) was defined as a heat-evoked change of the total chemical potential of all little loops upon a temperature-dependent change in the total enthalpy included in non-covalent crosslinking interactions from a fully closed state to a fully open state along the same gating pathway of one subunit within 10 °C, the mean Ω_{10} was also comparable to the functional thermo-sensitivity (Q_{10}), which was defined as the ratio of rates or open probabilities (P_o) measured 10°C apart. Taken together, these comparative results were consistent with three proposals. First, the melting temperature (T_m) of the biggest little loop may be responsible for the specific temperature threshold (T_{th}) for TRPV1 activation; Second, the balance between the open and inactivated states may determine the heat efficacy and the use-dependent desensitization; Third, the functional thermostability Q_{10} of TRPV1 may be controlled by the defined structural thermo-stability Ω_{10} in a PI lipid-dependent manner.

2. RESULTS

2.1. The Closed PI-free rTRPV1 at 25 °C had the Biggest Little Loop$_{21}$ in the VSLD/Pre-S1 interface

The previous chimera studies between rTRPV1 and rTRPV2 demonstrated that the transmembrane segment 434-687 and the pre-S1 segment 401-415 may be involved in the regulation of the temperature threshold while the pre-S1 segment 358-434 plays a critical role in mediating the temperature sensitivity Q_{10}. In contrast, an exchange of the C-terminal segment 688-838 has no effect. [17] On the other hand, the prior chimera investigations between TRPV1 and TRP melastatin 8 (TRPM8) indicated that the C-terminal including the TRP domain (693-710) is required for the polarity of thermal sensitivity. [21] Therefore, the segment from D388 in the pre-S1 domain to K710 in the TRP domain should be at least included as the gating pathway for the temperature threshold and sensitivity. At 25 °C, several kinds of non-covalent crosslinking interactions between amino acid side chains along this gating pathway of rTRPV1 formed a biophysical network of little topological loops in the closed state (**Fig.1A**).

First, H-bonds between different hydrophilic amino acid side chains contributed to the formation of little loops. In the pre-S1/VSLD interface, Q423-D427 and D424-R428 were paired for H-bonding. In the VSLD, T449-W549, R455-Y537-K535-Y463 and Q519-N551 were H-bonded in between. In the VSLD/S4-S5 linker/TRP/VSLD interfaces, the H-bonding pairs were R491-E709, R557-T704 and Q560-K694. In the pore domain and its interface with the TRP domain, pairs D576-T685, Y584-T641 and Q691-N695 were also engaged in H-bonds (**Fig. 1A**).

Second, aromatic π interactions also brought about little loops. Most of them were located in the VSLD and its interfaces with the pre-S1 domain. For example, Y401-R499-Y495, F434-W426/F438/Y555, F438-Y555, Y441-F488/F516/Y555, Y444-F448/F488, M445-W549, Y453-Y454, P456-Y463, V486-F490, Y487-F488/R491, F488-F516, F489-I493/L524, Y495/F517-F496, Y511-L515, F516-N551/Y554, F517-L521, F522-F543, Y530-F531/Y537 and Y554-Y555. In the S4-S5 linker/TRP interface, Q560 formed a CH-π interaction with W697. In the pre-S1/TRP interface, R701 produced a cation-π interaction with W426. In the pore domain, the π-interacting pairs had F580-L678, F589-T593, F591/T670-Y666, Y627/E636-F649, F640-Y666, and F649/Y653-F659 (**Fig. 1A**).

Third, salt bridging pairs included K425-E709 in the pre-S1/TRP interface, R491-E513 and R534-E536 in the VSLD, E648-K656 in the outer pore, and K688-E692 in the S6/TRP interface (**Fig. 1A**).

Taken together, along the gating pathway from D388 to K710, sixty non-covalent crosslinking interactions produced the total number of minimal lengths of little loops as 83 (**Fig. 1A**). Among the multiple little loops, although several smaller ones had 0 to 9 minimal residues in the loops, the biggest one was outstanding in the pre-S1/VSLD interface. It had a minimal 21-residue loop from Y401 to Q423, D427, W426, F434, Y555, Y441, F516, F517, F496, Y495, R499 and back to Y401 to control the R499-Y401 π interaction (**Figs. 1B-D**). Because two equivalent H-bonds sealed this biggest little $Loop_{21}$, the predicted melting temperature was about 32 °C (**Table 1**).

Table 1 New parameters of the rTRPV1 bio-thermometer based on the loop thermodynamic model

Construct	**Control**	**rTRPV1**			
Lipid environment	MSP2N2	MSP2N2			native
PDB ID	7LPE	7LPB	7LPD	7LPC	7LPC
Lipid PI at the capsaicin site	free	free	free	bound	bound
Sampling temperature, °C	**48**	**25**	**48**	**48**	
Gating state	open	closed	inactivated	closed	closed
Name of the biggest little loop	$Loop_9$	$Loop_{21}$	$Loop_{9'}$	$Loop_8$	$Loop_{13}$
Biggest little loop length (L_{max})	9	21	9	8	13
Equivalent H-bonds in L_{max}	1.0	2.0	2.0	2.0	1.5
Total non-covalent interactions	46	60	62	67	65
Total little loop lengths, a.a.	66	83	64	86	88
Calculated T_m, °C	46	**32**	56	**58**	**43**
Measured threshold T_{th}, °C	**>46**	**<48**		**>48**	**42**
Calculated $\Omega_{10,\,min}$ at E=0.5 kJ/mol		6.56	-0.60	10.5	10.9
Calculated $\Omega_{10,\,mean}$ at E=1.0 kJ/mol		**16.2**	**-1.0**	**28.8**	**28.7**
Calculated $\Omega_{10,\,max}$ at E=3.0 kJ/mol		67.4	-2.25	143	134
Measured Q_{10}		**16.4**			**28.2**
References for T_{th} and Q_{10}	[14]	[14]			[14]

2.2. PI-free rTRPV1 Opened at 48 °C with the Melting of the Biggest Little $Loop_{21}$ in the VSLD/pre-S1 Interface

If the biggest little $Loop_{21}$ with a minimal 21-residue length in rTRPV1 carries out the single-step melting reaction like DNA hairpins, the calculated melting temperature 32 °C should be enough to open it above 32 °C (**Table 1**). In agreement with this assumption, when PI-free rTRPV1 opened at 48 °C, the broken Y401-R499 π interaction resulted in the melting of the biggest little $Loop_{21}$ in the VSLD/pre-S1 interface with several changes along the gating pathway.

In the pre-S1/VSLD/TRP interfaces, the K425-E709 salt bridge and the Q423-D427 and D424-R428 and R491-D707 H-bonds were disconnected. In the VSLD/S4-S5 linker/TRP interfaces, when the Y554-Y555 π interaction was disrupted, the H-bond moved from R557-T704 to Y554-T704 and the π interaction shifted from Y555-F438 to F559-F438. When the Q560-K694 H bond was disrupted, the R557-E570 H-bond and the W697-R701 CH-π interaction were formed (**Fig. 2A**).

When this conformational change extended to the VSLD, the R491-E513 and R534-E536 salt bridges, the R455-Y537-K535-Y463 and Q519-N551 H-bonds, and the Y441/F516-F488 and F489-I493 and Y530-F531 π interactions were disconnected. In the meanwhile, the new Y495-R499/S510 H-bonds and the new R499-D509 salt bridge and the new F489-F490 π interaction emerged.

When this conformational change extended to the pore domain and its interfaces with the S4-S5 linker and the TRP domain, the E648-K656 and K688-E692 salt bridges and the Q691-N695 H-bond were disrupted. In the meanwhile, the new Y584-Y666 and T650-N652 and Y653-K656 H-bonds and the new E651-K656 salt bridge were born.

By all accounts, the total numbers of all non-covalent crosslinking interactions and minimal lengths of little loops along the gating pathway from D388 to K710 dramatically decreased from 60 and 83 to 46 and 66, respectively (**Fig. 2A**). As a result, the mean structural thermo-sensitivity Ω_{10} was about 16.2, which was similar to the experimental Q_{10} value 16.4 (**Table 1**). [14] On the other hand, even if one equivalent H-bond sealed the biggest little $Loop_9$ with a minimal 9-residue length in the VSLD/S4-S5 linker/TRP interfaces to control the stimulatory R557-E570 H-bond, the melting temperature was about 46 °C (**Fig. 2C, Table 1**).

2.3. PI-free rTRPV1 Inactivated at 48 °C with the Biggest Little $Loop_{9'}$ in the Pore Domain

When the H-bond moved from R557-E570 to E570-Q700 in the S4-S5 linker/TRP interface at 48 °C, the little $Loop_1$ with a minimal 1-residue length replaced the biggest little $Loop_9$ to stabilize the R557-E570-Q700 H-bonds up to a melting temperature 62 °C. As a result, the W697-R701 CH-π interaction became a strong cation-π interaction. Of special note, the formation of the H410-E692 π interaction and the N695-H410 and Y401-D707 H-bonds in the pre-S1/TRP interface locked the channel in a new state with other changes (**Figs. 3A-C**).

When the F559-F438 π interaction was broken in the S4-S5 linker/VSLD interface, the Y401-E397/R499 π interactions were present in the pre-S1/VSLD interface. In the VSLD, the F489-F490 and Y495-F496 and F517-F496/L521 π interactions were disrupted with the R499-D509 salt bridge and the Y495-S510 H-bond. In the meanwhile, the F438-Y555 and Y441-F488 and P456-Y463 and F489-I493/L524 and Y530-F531 and Y554-Y555 π interactions and the Y463-K535 H-bond and the R534-E536 salt bridge were restored with the new Y444-Q519 and Y463-Y537 and R491-Q494 H-bonds. Finally, in the outer pore, the E636-K639 salt bridge changed to an H-bond and the H-bonding pair moved from T650-N652 to E651-Y653 (**Fig.3A**).

Taken together, although the total number of all non-covalent crosslinking interactions along the gating pathway from D388 to K710 increased significantly from 46 to 62, the total number of the minimal lengths of little loops slightly decreased from 66 to 64 residues (**Fig. 3A**). However, the high melting temperature 62 °C prevented the E570-Q700 H-bond in the $Loop_1$ from being melted at 48 °C before the open state (Fig. 3B). Therefore, this new state was much more like a closed state but more stable than the open state and thus served as an inactivated state after the open state to desensitize the channel activity (**Figs. 1A, 2A, 3A**). In this case, a smaller little $Loop_2$ with a minimal 2-residue length from Y401 to T499, Y495, Q494, R491, Y487, F488, F516, Y554, T704, D707 and back to Y401 may be involved in the inactivation (**Figs. 3A, C, E**). On the other hand, another loop with a minimal 9-residue length from D576 to F580, L678, T685 and back to D576 in the S5-S6 interface became the biggest little $Loop_{9'}$ (**Figs. 3D-E**). When two equivalent H-bonds sealed it, the resultant melting temperature was about 56 °C (**Table 1**).

2.4. The Binding of PI to the Vanilloid Site Increased the Temperature Threshold and Sensitivity of rTRPV1

When the resident PI occupies the well-known vanilloid site, rTRPV1 in MSP2N2 cannot open even at 48 °C. This closed state of PI-bound rTRPV1 is almost identical between 4 °C and 48 °C. [14] However, once the PI lipid linked R409, D509, R557, E570 and Q700 together via H-

bonds, there were several differences between PI-bound rTRPV1 at 48 °C and PI-free rTRPV1 at 25 °C (**Figs. 4A-B**).

In the pore domain and its interfaces with the S4-S5 linker and the TRP domain, the E648-K656 and K688-E692 salt bridges were disrupted with the formation of the D576-R579 and Y627-E636-K639 and E692-R575 H-bonds, the K571-E570/E692 salt bridges and the D654-F655 π interaction. In the VSLD, the R491-E513 salt bridge, the R455-Y537-K535 H-bonds, and the F434-F438 and V486-F490 and F489-I493 and Y495-F496/R499 and Y511-L515 π interactions were disrupted. In the meanwhile, the Y441-Y444 and Y463-Y530 and F489-F490 and Y495-E513 π interactions were formed with the Y487-R491 π interaction changing to an H-bond (**Figs. 4A**).

In the VSLD/TRP interface, when the H-bond shifted from R557-T704 to Y554-T704, the R491-D707 H-bond was disconnected. In the S4-S5 linker/TRP interface, the Q560-K694 H-bond was also broken but the W697-R701 CH-π interaction appeared. In the pre-S1/TRP interfaces, the new E397-K710 and Y401-D707 and D411-N695 and Q423-R701 H-bonds and the new H410-I696 π interaction were added. Finally, in the pre-S1/VSLD interface, the Q423-D427 and D424-R428 H-bonds were disrupted with the Y401-R499 CH-π interaction becoming a cation-π interaction (**Figs. 4A**). In this case, the total numbers of the non-covalent crosslinking interactions and minimal lengths of little loops along the gating pathway were 67 and 86, respectively. If the same open state was employed as a control, the mean structural thermo-sensitivity Ω_{10} would be about 28.8, which was comparable to the Q_{10} value 28.2 (**Table 1**). [14] However, the tight interaction of rTRPV1 with MSP2N2 allowed the PI pocket to be the biggest little $Loop_8$ with a minimum 8-atom length (**Fig. 4B**). When two equivalent H-bonds sealed this loop, the calculated melting temperature was about 58 °C (**Table 1**). That may be why the PI-bound rTRPV1 in MSP2N2 cannot open at 48 °C [14]

Once the E697-K710 and Y401-D707 H-bonds had been broken in a normal lipid environment, the biggest little $Loop_{13}$ with a minimal 13-residue length from Y401 to R409, D509, E513, Y495 and R499 and back to Y401 would provide a melting temperature 42 °C as a normal threshold to disrupt the Y401-R499 π interaction and the related R409-D509 salt bridge so as to release the nearby PI lipid from the vanilloid site for rTRPV1 opening (**Table 1, Figs. 4A-D**). In that case, the total numbers of the non-covalent crosslinking interactions and minimal lengths of little loops along the same gating pathway would be 65 and 66, respectively. If the same open

state had been employed as a control, the mean structural thermo-sensitivity Ω_{10} would be about 28.7, which was also comparable to the Q_{10} value 28.2 (**Table 1**). [14]

3. DISCUSSION

TRPV1 is designed and created as a bio-thermometer in the thermostable system to detect noxious heat and to protect human or animal bodies from heat damage. [1-4] To this end, it should meet several protein engineering requirements. First, it should be an integral membrane protein with a relative high physicochemical stability or heat capacity to avoid thermal denaturation. Second, it should be an ion channel that can directly couple a temperature signal to an electronical signal reporter for a readout by a primary afferent sensory neuron. Third, its opening from the closed state within 10 °C apart should have a high Q_{10} with a steep response to a small change in a surrounding predetermined temperature. Fourth, it should have a heat switch with two temperature threshold limits for two gating states, one for activation to sense noxious heat and the other for inactivation to alleviate pain by exploiting the use-dependent desensitization upon constant or repeated noxious heat stimuli. In the biochemical and biophysical world, a little topological loop structure may be an ideal tool for thermosensitive TRP channels to achieve them.

The DNA hairpin loop with the limited lengths has been designed as a temperature switch, a thermometer and an ionic detector with Q_{10} in the range from 1.8 to 2.7. [20] Its oligonucleotides with complementary nucleotide sequences at the ends form a duplex region as the hairpin stem upon intra-strand hybridization, and its nucleotides in between as the hairpin loop. When a temperature increases above a threshold, the DNA hairpin melts and thus becomes single stranded. Its melting temperature threshold sharply depends on the H-bonded and stacked base pairs in the stem, the length and flexibility of the loop and the ionic strength in a solution. Generally, a stable stem or a small and rigid loop or a high salt concentration in the solution allows the DNA hairpin to have a high threshold to sense and to respond to highly specific and small changes in an environmental temperature. When the loop length is decreased from 20 to 10 A's or the H-bonded G-C base-pairs raise from 2 to 4, the melting temperature threshold can be increased more than 20 degrees. Clearly, a short stem favors sharp hairpin melting rather than gradual melting. Since a change in the loop sequence has no significant effect on the temperature threshold of the DNA biosensor, [20] once noncovalent crosslinking interactions in a single subunit create a single topological loop, the loop thermodynamics should be comparable between DNA and protein.

Like the DNA hairpin thermal biosensor, at a given physiological salt concentration (150 mM NaCl), when non-covalent crosslinking interactions made the biggest with the relatively longest path among little loops along the gating pathway from D388 in the pre-S1 domain to K710 in the TRP domain of rTRPV1, the melting temperature T_m increased with a decreased length and an increased number of equivalent H-bonds to seal the loop. In the absence of the PI lipid at the vanilloid site, rTRPV1 had the biggest little $Loop_{21}$ with a minimal 21-residue length from Y401 to Q423, D427, W426, F434, Y555, Y441, F516, F517, F496, F495, R499 and back to Y401 in the pre-S1/VSLD interface to control the Y401-R499 π interaction (**Fig. 1**). As two equivalent H-bonds kept this $Loop_{21}$, the melting temperature T_m was about 32 °C (**Table 1**). Therefore, its melting at 48 °C further disrupted the R499-Y401 π interaction in the loop and resulted in the formation of the biggest little $Loop_9$ with a minimal 9-residue length from R557 to E570, Q560, W697, R701, Q700 and back to R557 (**Fig. 2**). However, the presence of one equivalent H-bond to control the R557-E570 H-bond set a melting temperature threshold T_{th} at about 46 °C (**Table 1**). Therefore, at 48 °C the formation of the E570-Q700 H-bond further generated the little $Loop_1$ with a 1-residue length to replace the $Loop_9$ for a higher melting temperature T_m 62 °C with one equivalent H-bond to seal the loop. In this case, the biggest little $Loop_{9'}$ appeared in the S5-S6 interface with a minimal 9-residue length from D576 to F580 and L678 and T685 and back to D576 (**Fig. 3**). This loop was sealed by two equivalent H-bonds so that the melting temperature T_m was about 56 °C (**Table 1**). On the other hand, in the absence of the E397-K710 and Y401-D707 H-bonds in a native lipid environment, the biggest little $Loop_{13}$ would have a normal melting temperature 43 °C in the presence of 1.5 equivalent H-bonds to seal a minimal 13-residue loop from Y401 to R409, D509, E513, Y495, R499 and back to Y401 (**Table 1, Figs. 4A, 4C, 4D**). Thus, the binding of PI to the vanilloid site may increase the temperature threshold from 32 °C to 43 °C in a normal lipid system. However, once PI-bound rTRPV1 was reconstituted in MSP2N2, the presence of those two H-bonds allowed the PI pocket at the vanilloid site to be the biggest little $Loop_8$ with 2 equivalent H-bonds to maintain a minimal 8-atom loop. The resultant melting temperature 58 °C could prevent the release of PI from the vanilloid site at 48 °C for channel opening (**Table 1, Figs. 4A, 4B, 4D**). Therefore, like a DNA hairpin, a single-step melting reaction of the biggest little topological loop may be rate-limiting for the specific temperature-dependent threshold (T_{th}) in rTRPV1. In accordance with this proposal, in the putative presence of the biggest little $Loop_{12}$ with a minimal 12-residue length from Y408 to R415, D517, E521, Y503, R507 and

back to Y408 (**Fig. 4D**), platypus (*Ornithorhynchus anatinus*) TRPV1 (pTRPV1) decreases an activation threshold by about 3 °C. [19]

Despite five biggest little loops in rTRPV1, their roles in gating states may be different. The $Loop_{21}$ may be closely coupled to the lower S6 gate via the R499-Y401 π interaction in the VSLD/pre-S1 interface. Therefore, its melting disrupted this non-covalent crosslinking bridge, allowing PI-free rTRPV1 to open above 32 °C (**Table 1, Figs. 1-2**). In contrast, the $Loop_9$ may favor the open state by uplifting the S4-S5 linker against the S6 gate via the stimulatory R557-E570 H-bond in the VSLD/S4-S5 linker interface. As the mutation R557E/A/L or E570L/A can disrupt the stimulatory R557-E570 H-bond, it is reasonable that the R557E or E570L mutant leads to a complete loss of function, or mutants R557A/L and E570A have low heat sensitivity, or E570A increases the threshold from 41.5 °C to 44.3 °C. [22, 23] Since the $Loop_9$ had one equivalent H-bond to seal a minimal 9-residue loop for the open state of rTRPV1 (**Figs. 2, 5A**), it had an upper melting temperature limit 46 °C. However, when another E570-Q700 H-bond decreased the minimal loop length from 9 residues to one residue for a higher melting temperature 62 °C to protect the R557-E570 H-bond from the disruption above 46 °C, TRPV1 was inactivated irreversibly below 62 °C. [18] In this case, the $Loop_{9'}$ appeared in the S5-S6 interface increasing the upper melting temperature limit from 46 °C to 56 °C (**Table 1**). Therefore, the upper threshold limit for the rTRPV1 bio-thermometer may be 56 °C. In the meanwhile, the presence of the E397-K710 and Y401-D707 H-bonds in the pre-S1/TRP interface may inactivate the channel, alleviating pain upon constant or repeated noxious heat stimuli-induced desensitization (**Table 1, Figs. 2-3**). [1, 8, 14, 18-19] In agreement with this proposal, the absence of a serine residue between S410 and E411 may not allow pTRPV1 to have E404-K718 and Y408-D715 H-bonds in the pre-S1/TRP interface to inactivate pTRPV1 (**Figs. 3E, 4D**). [19] In this regard, the deletion of S404 or the D707A mutation may stop inactivation of rTRPV1, and the cryo-EM structure of pTRPV1 may have unique closed and open states but not an inactivated state around 40 °C in the presence of 150 mM NaCl.

On the other hand, in the native lipid system, the putative biggest little $Loop_{13}$ with a minimal 13-residue length in the VSLD/pre-S1 interface may have a normal melting temperature 42 °C (**Table 1, Figs. 4C-D**). Like the $Loop_{21}$, its melting above 42 °C may disrupt the R499-Y401 π interaction in favor of channel opening (**Fig. 5A**). When the salt concentration was lowered down from 150 mM to 130 mM, the threshold may also decrease from 42 °C to 37.7 °C.

[8, 19] However, when rTRPV1 was reconstituted in MSP2N2, the biggest little $Loop_8$ had a minimal 8-atom length in the PI pocket to prevent PI from release below 58 °C. The very high melting temperature in such a lipid system may be beyond the physiological range for the detection of noxious heat unless a vanilloid compound like capsaicin could bind near D509 and R557 to compete off the PI lipid (**Table 1, Fig. 4**). [14] Taking all these into account, rTRPV1 may have a bio-thermometer range from 42 °C to 56 °C to monitor the noxious heat (**Fig.5A**). Further experiments are necessary to examine the role of the Y401-R499 π interaction and the R409-D509 salt bridge in securing the normal temperature threshold 42 °C for rTRPV1 opening.

In addition to five biggest little loops, five smallest little loops with a 0-residue length may also be required for channel gating. The first from Y444 to M445, W549, T449, F448 and back to Y544 was highly conserved in the VSLD of all the gating states and thus may serve as a static anchor (**Figs. 1-5**). The second from Y441 and through F516 and Y554 and Y555 and back to Y441 in the VSLD was shared by both closed and open states (**Figs 1-2, 5B**), and the related aromatic residues were highly conserved in thermosensitive TRPV1-4 but not in non-thermosensitive TRPV5-6. [11, 24] The tight π interactions may allow both smallest little loops to serve as relatively stationary anchors against which the S4–S5 linker can uplift in favor of TRPV1 opening. In support of this notion, the Y441S, Y444S, M445W, Y554A or Y555S mutation leaves the channel not functional. [22, 25] The third linked W426 on pre-S1, F434 and F438 on S1, F559 and Q560 in the S4-S5 linker, and W697 and R701 in the TRP domain together. This little $Loop_0$ may play a critical role in stabilizing the open state (**Figs. 2, 5B**). The fourth from Y584 to T641 and F640 and Y666 and back to Y584 was present in the pore domain of the open and desensitized states. (**Fig. 5B**). The residues for this smallest little $Loop_0$ were also highly conserved in TRPV1-4 but not in TRPV5-6. [11, 24] In agreement with its importance, the Y666A mutation is not functional while the F640L or T641S mutation decreases the temperature threshold to allow either to be constitutively active at room temperature. [26-27] The fifth may stabilize the open state by linking F649, F659, Y653, K656, E651, N652, T650 together against a highly-conserved anchor $Loop_8$ from Y627 to F649 and E636 and back to Y627 in the pore domain (**Figs. 2A, 5B**). It has been reported that the N628K or N652T or Y653T or combined mutation increases the temperature threshold, and the triple mutant N628K/N652T/Y653T has the longer opening durations [7] Furthermore, the N628L mutation greatly decreases the heat sensitivity (Q_{10} ~ 2.6) but the N628D mutation has the opposite effect (Q_{10} ~ 86), [14] possibly by mediating the thermal

stability of these two smaller little loops through ionic interactions with nearby E636. On the other hand, the turret deletion or replacement with glycine between G603 and N626 in mouse TRPV1 (mTRPV1) decreases the temperature threshold to a different extent, [8] possibly by weakening the corresponding R500-Y402 π interaction in the VSLD/pre-S1 interface or generating another new biggest little loop with a minimal length larger than 13 residues in the loop along the gating pathway from D389 to K711. Notably, although the deletion of the turret (Δ604-626) still allows the TRPV1 mutant construct to be activated by heat, the binding of external double-knot toxin or vanilla-toxin (DkTX) to the outer pore prevents heat activation, [9, 15] possibly by affecting the little loops in the outer pore (**Fig.5**).

Finally, the little $Loop_6$ had a minimal 6-residue length from D576 to K579 and F580 and L678 and T685 via the D576-T685 and D576-R579 H-bonds and the F580-L678 CH-π interaction (**Fig. 4A**). The D576-R579 H-bond was disrupted in the open state (**Fig. 2**). It has been reported that the mutant R579E is not functional and the D576N/R or R579A mutant is less sensitive to heat than wild type rTRPV1. [22] Since the residues for this smaller little $Loop_6$ are conserved in TRPV1-6, it may serve as a key common anchor in the pore domain. [11, 24] Thus, both the biggest and smaller little loops may be important for heat activation of TRPV1.

When non-covalent crosslinking interactions form a biophysical network in a bio-macromolecule, the dissociation rate (k_d) of enthalpy-driven crosslinks is accelerated at elevated temperatures but k_d of entropy-driven crosslinks is negligibly affected or even slowed under these conditions. [30] Since the temperature threshold for TRPV1 opening was determined by a rate-limiting single step to disrupt a non-covalent crosslinking interaction in the biggest little loop along the gating pathway (**Table 1**), and the opening rate or the open probability (P_o) of TRPV1 increases at raised temperatures, [18, 31] TRPV1 opening is enthalpy-driven ($\Delta H<0$). When PI-free rTRPV1 opens at 48 °C from a closed state at 25 °C, the opening of multiple little loops may increase entropy but decrease enthalpy as a result of the decrease in the total non-covalent crosslinking interactions from 60 to 46 along the gating pathway from D388 to K710 (**Figs 1-2**). [28] Thus, a small decrease in the Gibbs free energy may be enough for intra-molecular gating rearrangements to activate TRPV1. However, even if several short little loop crosslinks were included, such a small decrease may be insufficient to produce a high Q_{10} for noxious heat detection. Therefore, a heat-induced decrease in the total chemical potential of all the little loops upon the heat-evoked decrease in the total enthalpy included in the non-covalent crosslinking

interactions along the same gating pathway from a closed state to an open state should be considered. In direct line with this proposal, when the total number of all minimal lengths of little loops dramatically decreased upon the decrease of the total non-covalent crosslinking interactions, the resultant mean structural thermo-sensitivity (Ω_{10}) was comparable to the functional thermo-sensitivity (Q_{10}). For PI-free rTRPV1, the calculated mean Ω_{10} was about 16.2 while the experimental Q_{10} is about 16.4. For PI-bound rTRPV1, the predicted mean Ω_{10} was about 28.7 while the experimental Q_{10} is 28.2. [1, 14] Thus, the presence of the PI lipid at the vanilloid site apparently increased both mean Ω_{10} and Q_{10} values by about 70%. [14] When the intensity of a non-covalent interaction ranged from the minimal 0.5 kJ/mol to the maximal 3 kJ/mol, the normal Ω_{10} could be in a range from 10.9-134 (**Table 1**). Therefore, any measured Q_{10} values may be reasonable in this range. [1, 8, 14, 17-19]

It should be noteworthy that even if heat-evoked TRPV1 opening is enthalpy-drive, an increase in the heat capacity as a result of rearrangements of little loops from a closed state to an open state along the same gating pathway may be necessary to secure a minimal decrease in the Gibbs free energy for channel opening with a maximal Q_{10} value. [29]

4. CLOSING REMARK

The little topological loops in an ion channel can be used to design a thermosensitive bio-thermometer with a high Q_{10} value. In addition to the ionic strength in the physiological range, the little loop length and the number and the intensity of the loop-forming non-covalent crosslinking interactions between amino acid side chains in a complex biochemical reaction network can be used to tune the little loop strength for different melting temperature thresholds to detect distinct small environmental temperature changes. These non-covalent crosslinking interactions include salt bridges, aromatic side chain π interactions and H-bonds. Both the biggest and smaller little loops are necessary to control channel gating and the related thermal efficacy. Their opening and closure should be reversible and fast enough to have a very large temperature-dependent effect on channel gating, which can be easily coupled to an electrical readout from the primary afferent sensor neuron. What is more, the use-dependent desensitization may use gating state-dependent thermostability as a protective measure against noxious heat damage. In this regard, this computational study may render a broad structural basis for thermosensitive TRP channels to work as a bio-thermometer. On the other hand, although a given non-covalent interaction's spatial and geometric requirements have been well-understood, it is still hardly

predictable in a complex temperature-dependent biochemical reaction network. In this regard, this loop thermodynamic model, once examined by the temperature-dependent structural data of TRPV1, may provide more creative metrics for identifying causal structure–activity/selectivity relationships in a supramolecular architecture at a variety of ambient temperatures.

5. METHODS

In this computational study, the little topological loops in rTRPV1 channels below and above the temperature thresholds were analyzed with graph theory as the bio-thermometer basis for noxious heat detection. The *in silico* protomer models were based on the cryo-EM structural data of closed rTRPV1 in MSP2N2 with PI-bound at 4 °C (PDB ID, 7LP9, model resolution= 2.63 Å) and 48 °C (PDB ID, 7LPC, model resolution= 3.07 Å), capsaicin-bound at 25 °C (PDB ID, 7LPB, model resolution= 3.54 Å) and 48 °C (PDB ID, 7LPD, model resolution= 3.55 Å), and open rTRPV1 with capsaicin-bound at 48 °C (PDB ID, 7LPE, model resolution= 3.72 Å), [14] UCSF Chimera was used to assess non-covalent crosslinking interactions in TRPV1. All the stereo- or regioselective diagonal and lateral non-covalent crosslinking interactions such as salt-bridges and lone pair/CH/cation-π interactions and H-bonds between amino acid side chains along the gating pathway from D388 in the pre-S1 domain to K710 in the TRP domain of rTRPV1 were included to test their potential roles in forming the little loops with minimal lengths to control the specific temperature thresholds for different gating states and to stablize the heat efficacy for the PI lipid-dependent temperature coefficient Q_{10}.

The standard definition of noncovalent crosslinking interactions was employed. A hydrogen bond was considered present when the angle donor-hydrogen-acceptor was within the cut-off of 60°, and when the hydrogen-acceptor distance is within 2.5 Å and the maximal distance is 3.9 Å between a donor and an acceptor. A salt bridge was considered to be formed if the distance between any of the oxygen atoms of acidic residues and the nitrogen atoms of basic residues were within the cut-off distance of 3.2-4 Å in at least one frame. When the geometry was acceptable, a salt bridge was also counted as a hydrogen bonding pair. The face-to-face π-π stacking of two aromatic rings was considered effective once the separation between the π-π planes was ~3.35-4.4 Å, which is close to at least twice the estimated van der Waals radius of carbon (1.7 Å). The edge-to-face π-π interaction of two aromatic rings was considered attractive when the cut-off distance between two aromatic centers was within 4-6.5 Å. Significant cation-π interactions occurred within a distance of 6.0 Å between a cation and an aromatic center. The short effective CH/π

distances was 2.65-3.01 Å between aromatic groups, and 2.75-2.89 Å between CH_3 and an aromatic ring. The lone pair-π interaction distance between a lone electron pair and an aromatic ring was within 3-3.7 Å. [32]

After non-covalent crosslinking interactions were scanned along the gating pathway of rTRPV1 from D388 in the pre-S1 domain to K710 in the TRP domain, graph theory was used as a novel tool to define little loops as those that had the minimal lengths to control non-covalent crosslinking interactions. All the temperature-dependent little loops with minimal lengths were geometrically mapped along the gating pathway in the closed, open and desensitized states. The primary amino acid sequence line from D388 to K710 was marked in black. An amino acid side chain or an atom of a bound lipid involving a non-covalent interaction along the gating pathway of rTRPV1 was represented as a vertex (*v*) or a node and marked with an arrow in different colors. The same kind of non-covalent crosslinking interactions was marked in the same color. Any link between two vertices was represented as an edge in a biochemical reaction network. A topological loop was formed between two vertices *i* and *j* (v_i and v_j), if and only if there was a path from v_i to v_j and a return path from v_j to v_i. The loop path length (L) was definded as the total number of residues in protein or atoms in the bound lipid that do not participate in any non-covalent crosslinking interctions in a loop. For a given biochemical reaction network, the minimal loop path length (L_{min}) between v_i and v_j was the sum of the shortest return path distance from node *j* to i because the direct shortest path distance from node *i* to *j* was zero when a non-covalent interaction existed between them. The simplest way to find the minimal loop length was to identify the shortest return path between two vertices *i* and *j* (v_i and v_j) by using the Floyd-Warshall algorithm. [33] For example, in the biochemical reaction network of Fig.1A, a direct path length from E636 and F649 was zero because there was a CH-π interaction between them. However, there was another shortest return path from F649 to Y627 and back to E636 via a π–π interaction. Therefore, the minimal little loop length was 8. After each non-covalent crosslinking interaction was tracked by a minimal loop length and the uncommon lengths were marked in black, a little loop with a minimal x-residue or atom length was named as $Loop_x$, and the total numbers of all noncovalent interactions and minimal lengths of little loops along the gating pathway of one subunit were shown in black and blue circles, respectively.

The temperature threshold (T_{th}) was calculated from a melting temperature T_m of the biggest little loop along the gating pathway using the following equation: [20]

$$T_m\ (°C) = 34 + (n-2)\times 10 + (20-L_{max})\times 2 \quad (1)$$

where, n is the total number of the non-covalent crosslinking interactions equivalent to H-bonds in the biggest little loop, and L_{max} is the length of the biggest little loop.

For enthalpy-driven TRPV1 opening, if a thermosensitive TRPV1 channel changes from a fully closed state to a fully open state within a temperature range ΔT, the structural thermo-sensitivity ($\Omega_{\Delta T}$) of a single ion channel can be defined and calculated using the following equations:

$$\Omega_{\Delta T} = [(L_c - L_o)E/2]^{(Hc/Ho)} = [(L_c - L_o)E/2]^{[(ENc)/(ENo)]} = [(L_c - L_o)E/2]^{(Nc/No)} \quad (2)$$

where, H_c and H_o are the total enthalpy included in non-covalent crosslinking interactions in the closed and open states along the same gating pathway of one subunit, respectively; N_c and N_o are the total numbers of all the non-covalent crosslinking interactions along the same gating pathway of one subunit in the closed and open states, respectively; L_c and L_o are the total numbers of all the minimal lengths of little loops along the same gating pathway of one subunit in the closed and open states, respectively. E is the energy intensity of a non-covalent crosslinking interaction in a range of 0.5-3 kJ/mol. Usually, E is 1 kJ/mol. [32] Thus, $\Omega_{\Delta T}$ reflects a heat-evoked change in the total chemical potential of little loops upon a heat-evoked change in the total enthalpy included in non-covalent crosslinking interactions from a closed state to an open state along the same gating pathway of one subunit.

When ΔT=10 °C, Ω_{10} could be comparable to the functional thermo-sensitivity (Q_{10}) of a single ion channel. Q_{10} was calculated using the following equation:

$$Q_{10} = (X_2/X_1)^{10/(T2-T1)} \quad (3)$$

where, X_1 and X_2 are open probability (P_o) values or reaction rates obtained at temperatures T1 and T2 (measured in kelvin), respectively.

Conventions and Abbreviations: cryo-EM, cryo-electron microscopy; DkTx, double-knot toxin or vanillotoxin; k_d, the dissociation rate; Ω_{10}, structural thermosensitivity; Q_{10}, functional thermo-sensitivity; PI, phosphatidylinositol; P_o, open probability; T_m, melting temperature; T_{th}, temperature threshold; TRP, transient receptor potential; TRPM8, TRP melastatin 8; TRPV1, TRP vanilloid-1; TRPVi (i=1; 2, 3, 4, 5, 6); hTRPV1, human TRPV1; mTRPV1, mouse TRPV1; pTRPV1, platypus TRPV1; rTRPV1, rat TRPV1; VSLD, voltage-sensor-like domain

References

1. Caterina, M.J. et al. The capsaicin receptor: a heat-activated ion channel in the pain pathway. *Nature* **389,** 816-824 (1997).
2. Davis, J. B. et al. Vanilloid receptor-1 is essential for inflammatory thermal hyperalgesia. *Nature* **405,** 183-187 (2000),
3. Gavva, N. R. et al., Pharmacological blockade of the vanilloid receptor TRPV1 elicits marked hyperthermia in humans. *Pain* **136**, 202-210 (2008).
4. Vandewauw, I. et al. A TRP channel trio mediates acute noxious heat sensing. *Nature*, **555,** 662-666 (2018**).**
5. Chung, M. K., Wang, S. Cold suppresses agonist-induced activation of TRPV1. *J Dent Res.* **90,** 1098-1102 (2011**)**.
6. Jordt, S. E., Julius, D. Molecular basis for species-specific sensitivity to "hot" chili peppers. *Cell* **108,** 421-430 (2002).
7. Grandl, J. et. al. A. Temperature-induced opening of TRPV1 ion channel is stabilized by the pore domain. *Nat Neurosci.* **13,** 708-714 (2010).
8. Cui, Y. et al. Selective disruption of high sensitivity heat activation but not capsaicin activation of TRPV1 channels by pore turret mutations. *J. Gen. Physiol.* **139,** 273-283 (2012).
9. Jara-Oseguera, A., Bae, C., Swartz, K. J. An external sodium ion binding site controls allosteric gating in TRPV1 channels. *Elife* **5,** (2016); 10.7554/eLife.13356.
10. Long, S. B., Campbell, E. B., Mackinnon, R. Crystal structure of a mammalian voltage-dependent Shaker family K^+ channel. *Science* **309**, 897-903 (2005).
11. Liao, M., Cao, E., Julius, D., Cheng, Y. Structure of the TRPV1 ion channel determined by electron cryo-microscopy. *Nature* **504,** 107-112 (2013).
12. Cao, E., Liao, M., Cheng, Y., Julius, D. TRPV1 structures in distinct conformations reveal activation mechanisms. *Nature* **504,** 113-118 (2013).
13. Nadezhdin, K. D. et al. Extracellular cap domain is an essential component of the TRPV1 gating mechanism. *Nat Commun.* **12,** 2154 (2021); 10.1038/s41467-021-22507-3.
14. Kwon, D. H. et al., Heat-dependent opening of TRPV1 in the presence of capsaicin. *Nat Struct Mol Biol*. **28,** 554-563 (2021).
15. Gao, Y., Cao, E., Julius, D., Cheng, Y. TRPV1 structures in nanodiscs reveal mechanisms of ligand and lipid action. *Nature* **534,** 347-351. (2016).

16. Wang, G. Lipid-dependent sequential allosteric activation of heat-sensing TRPV1 channels by anchor-stereoselective “hot” vanilloid compounds and analogs. *Biochem. Biophys. Rep*. **28,** 101109. (2021); 10.1016/j.bbrep.2021.101109.
17. Yao, J., Liu, B., Qin, F. Modular thermal sensors in temperature-gated transient receptor potential (TRP) channels. *PNAS* **108,** 11109‑11114 (2011).
18. Sa´nchez-Moreno, A. et al. Irreversible temperature gating in trpv1 sheds light on channel activation *eLife* **7,** e36372 (2018); 10.7554/eLife.36372.
19. Luo, L. et al. Molecular basis for heat desensitization of TRPV1 ion channels. *Nat Commun.* **10,** 2134 (2019); 10.1038/s41467-019-09965-6. Correction in: *Nat Commun*. **11,** 1798 (2020); 10.1038/s41467-020-15691-1.
20. Jonstrup, A. T., Fredsøe, J., Andersen, A. H. DNA hairpins as temperature switches, thermometers and ionic detectors. *Sensors* **13,** 5937-5944 (2013).
21. Brauchi, S,, Orta, G., Salazar, M., Rosenmann, E., Latorre, R. A hot-sensing cold receptor: C-terminal domain determines thermosensation in transient receptor potential channels. *J Neurosci.* **26,** 4835–4840 (2006).
22. Boukalova, S., Marsakova, L., Teisinger, J., Vlachova, V. Conserved residues within the putative S4–S5 region serve distinct functions among thermosensitive vanilloid transient receptor potential (TRPV) channels. *J. Biol. Chem*. **285,** 41455-41462 (2010).
23. Kim, M. et al. Evidence that the TRPV1 S1-S4 membrane domain contributes to thermosensing. *Nat Commun.* **11,** 4169 (2020); 10.1038/s41467-020-18026-2.
24. Nadezhdin, K. D. et al. Structural mechanism of heat-induced opening of a temperature-sensitive TRP channel. *Nat. Struct. Mol. Biol.* **28,** 564–572 (2021).
25. Boukalova, S., Teisinger, J., Vlachova, V. Protons stabilize the closed conformation of gain-of-function mutants of the TRPV1 channel. *Biochim. Biophys. Acta*. **1833,** 520-528 (2013).
26. Susankova, K., Ettrich, R., Vyklicky, L., Teisinger, J., Vlachova, V. Contribution of the putative inner-pore region to the gating of the transient receptor potential vanilloid subtype1 channel (TRPV1). *J. Neurosci.* **27,** 7578-7585 (2007).
27. Myers, B. R., Bohlen, C. J., Julius, D. A. yeast genetic screen reveals a critical role for the pore helix domain in TRP channel gating. *Neuron* **58,** 362-373 (2008).
28. Kiehna, S. E., Waters, M. L. Sequence dependence of β-hairpin structure: Comparison of a salt bridge and an aromatic interaction. *Protein Science* **12,** 2657-2667 (2003).

29. Clapham, D. E., Miller, C. A thermodynamic framework for understanding temperature sensing by transient receptor potential (TRP) channels. *PNAS* **108,** 19492–19497 (2011).
30. Yu, A. C. et al. Physical networks from entropy-driven non-covalent interactions *Nat Commun*. **12,** 746 (2021); 10.1038/s41467-021-21024-7.
31. Sun, X. Zakharian, E. Regulation of the temperature-dependent activation of transient receptor potential vanilloid 1 (TRPV1) by phospholipids in planar lipid bilayers. *J. Biol. Chem.* **290,** 4741–4747 (2015).
32. Neel, A. J., Hilton, M. J., Sigman, M. S. Toste, F. D. Exploiting non-covalent π interactions for catalyst design. *Nature* **543,** 637-645 (2017).
33. Floyd, R. W. Algorithm-97 - Shortest path. *Commun Acm*, **5,** 345–345 (1962).

Acknowledgements

The author's own studies cited in this article were supported by NIDDK Grant (DK45880 to D.C.D.) and Cystic Fibrosis Foundation grant (DAWSON0210) and NIDDK grant (2R56DK056796-10) and American Heart Association (AHA) Grant (10SDG4120011 to GW).

Author contributions

G. W. wrote the main manuscript text, prepared table 1 and figures 1-5, and reviewed the whole manuscript.

Data availability statement: All data generated or analysed during this study are included in this published article.

Competing interests

The author declares no conflict of interest.

Figure legends

Figure 1. **The little topological loop network along the gating pathway of PI-free rTRPV1 in the closed state at 25 °C. A,** The little topological loop map. The cryo-EM structure of one subunit in closed rTRPV1 with capsaicin bound at 25 °C (PDB ID, 7LPB) was used for the model.[14] The pore domain, the S4-S5 linker, the TRP domain, the VSLD and the pre-S1 domain are indicated in black. Salt bridges, π interactions, and H-bonds between pairing amino acid side chains along the gating pathway from D388 to K710 are marked in purple, green, and orange, respectively. The minimal lengths of little loops required to control the relevant non-covalent crosslinking interactions were calculated with graph theory and labeled in black. The total numbers of all minimal loop lengths and loop-forming non-covalent crosslinking interactions along the gating pathway are shown in the blue and black circles, respectively. **B,** The location of the biggest little $Loop_{21}$ in the pre-S1/VSLD interface. **C,** The structure of the biggest little $Loop_{21}$ with a minimal 21-residue length in the VSLD/pre-S1 interface to control the Y401-R499 π interaction. **D,** The sequence of the biggest little $Loop_{21}$ to control the R499-Y401 π interaction in the blue box.

Figure 2. **The little topological loop network along the gating pathway of PI-free rTRPV1 in the open state at 48 °C. A,** The little topological loop map. The cryo-EM structure of one subunit in open rTRPV1 with capsaicin bound at 48 °C (PDB ID, 7LPE) was used for the model.[14] The pore domain, the S4-S5 linker, the TRP domain, the VSLD and the pre-S1 domain are indicated in black. Salt bridges, π interactions, and H-bonds between pairing amino acid side chains along the gating pathway from D388 to K710 are marked in purple, green, and orange, respectively. The minimal lengths of little loops required to control the relevant non-covalent crosslinking interactions were calculated with graph theory and labeled in black. The total numbers of all minimal loop lengths and loop-forming non-covalent crosslinking interactions along the gating pathway are shown in the blue and black circles, respectively. **B,** The structure of the smalles little $loop_0$ with a zero-residue length in the VSLD to replace the R499-Y401 π interaction with the R499-D509 salt bridge. **C,** The structure of the biggest little $Loop_9$ with a minimal 9-residue length in the VSLD/S4-S5 linker/TRP interfaces to control the stimulatory R557-E570 H-bond. **D,** The

sequences of little $Loop_0$ and $Loop_9$ with minimal 0- and 9-residue lengths to control the R499-D509 salt bridge and the R557-E570 H-bond in the blue boxes, respectively.

Figure 3. **The little topological loop network along the gating pathway of PI-free rTRPV1 in the desensitized state at 48 °C. A,** The little topological loop map. The cryo-EM structure of one subunit in inactivated rTRPV1 with capsaicin bound at 48 °C (PDB ID, 7LPD) was used for the model.[14] The pore domain, the S4-S5 linker, the TRP domain, the VSLD and the pre-S1 domain are indicated in black. Salt bridges, π interactions, and H-bonds between pairing amino acid side chains along the gating pathway from D388 to K710 are marked in purple, green, and orange, respectively. The minimal lengths of little loops required to control the relevant non-covalent crosslinking interactions were calculated with graph theory and labeled in black. The total numbers of all minimal loop lengths and loop-forming non-covalent crosslinking interactions along the gating pathway are shown in the blue and black circles, respectively. **B,** The structure of the little $Loop_1$ with a 1-residue length in the VSLD/S4-S5 linker/TRP/VSLD interfaces to govern the R557-E570 H bond. **C,** The structure of the putative little $Loop_2$ in the VSLD/pre-S1/TRP/VSLD interfaces to control the Y401-D707 H-bond for inactivation and desensitization. **D,** The structure of the biggest little $Loop_9$ with a minimal 9-residue length in the S5-S6 interface to control the D576-T685 H-bond. **E,** The sequences of little $Loop_1$, $Loop_2$, $Loop_9$ with minimal 1-, 2-, and 9-residue lengths to control the R557-E570 and Y401-D707 and D576-T685 H-bonds in the blue rectangles, respectively.

Figure 4. **The little topological loop network along the gating pathway of PI-bound rTRPV1 in the closed state at 48 °C. A,** The little topological loop map. The cryo-EM structure of one subunit in closed rTRPV1 with PI bound at 48 °C (PDB ID, 7LPC) was used for the model.[14] The pore domain, the S4-S5 linker, the TRP domain, the VSLD and the pre-S1 domain are indicated in black. Salt bridges, π interactions, and H-bonds between pairing amino acid side chains along the gating pathway from D388 to K710 are marked in purple, green, and orange, respectively. The minimal lengths of little loops required to control the relevant non-covalent crosslinking interactions were calculated with graph theory and labeled in black. The total numbers of all minimal loop lengths and loop-forming non-covalent crosslinking interactions along the gating pathway are shown in the blue and black circles, respectively. The dashed lines

are absent in the native lipid system. The putative little loop lengths in the native lipid system are labled in grey. **B,** The structure of the biggest little $Loop_8$ with a minimal 8-atom length for the PI pocket. **C,** The structure of the biggest little $Loop_{13}$ with a minimal 13-residue length in the VSLD/pre-S1 interface to control the Y401-R499 cation-π interaction near PI. **D,** The sequences of the biggest little $Loop_8$, $Loop_{13}$, $Loop_{12}$ with minimal 8-carbon, 13-residue, and 12-residue lengths to control the PI pocket in rTRPV1, the Y401-R499 π interaction in rTRPV1, and the Y408-R507 π interaction in pTRPV1, respectively. The controlled bridges are marked in the blue rectangles.

Figure 5. The tentative model for TRPV1 opening and desensitization upon the heat-evoked melting of the biggest little loops. A. The homo-tetrameric cryo-EM structures of rTRPV1 in the closed and open and desensitized states (PDB ID: 7LP9, 7LPE, 7LPD, respectively) were used for the model. [14] For a convenient view, only two subunits are shown. The dashed rectangle is the membrane area. In the presence of the PI lipid (blue) at the capsaicin site, rTRPV1 has 1.5 equivalent H-bonds (orrange) to seal the biggest little $Loop_{13}$ (red) with a minimal 13-residue length (red) in the VSLD/pre-S1 interface so that rTRPV1 is closed below a threshold 42 °C. When the temperature increases above the threshold 42 °C, rTRPV1 is open upon the melting of the biggest little $Loop_{13}$ in the VSLD/pre-S1 interface. In the meantime, the biggest little $Loop_9$ (red) with a minimal 9-residue length (red) and one equivalent H-bond (orrange) is formed in the VSLD/S4-S5 linker/TRP/VSLD interfaces in favor of the open state. However, the open state is unstable. The shrinking of $Loop_9$ further inactivates and desensitizes rTRPV1 in a temperature range from 42 °C to 56 °C. In the desensitized state, the little $Loop_{9'}$(red) with a minimal 9-residue length (red) and two equivalent H-bonds (orrange) in the S5-S6 interface becomes the biggest with a melting temperatrure 56 °C. **B,** The proposed smaller little loops for TRPV1 gating. The minimal loop lengths are shown in the red circles.

Figures

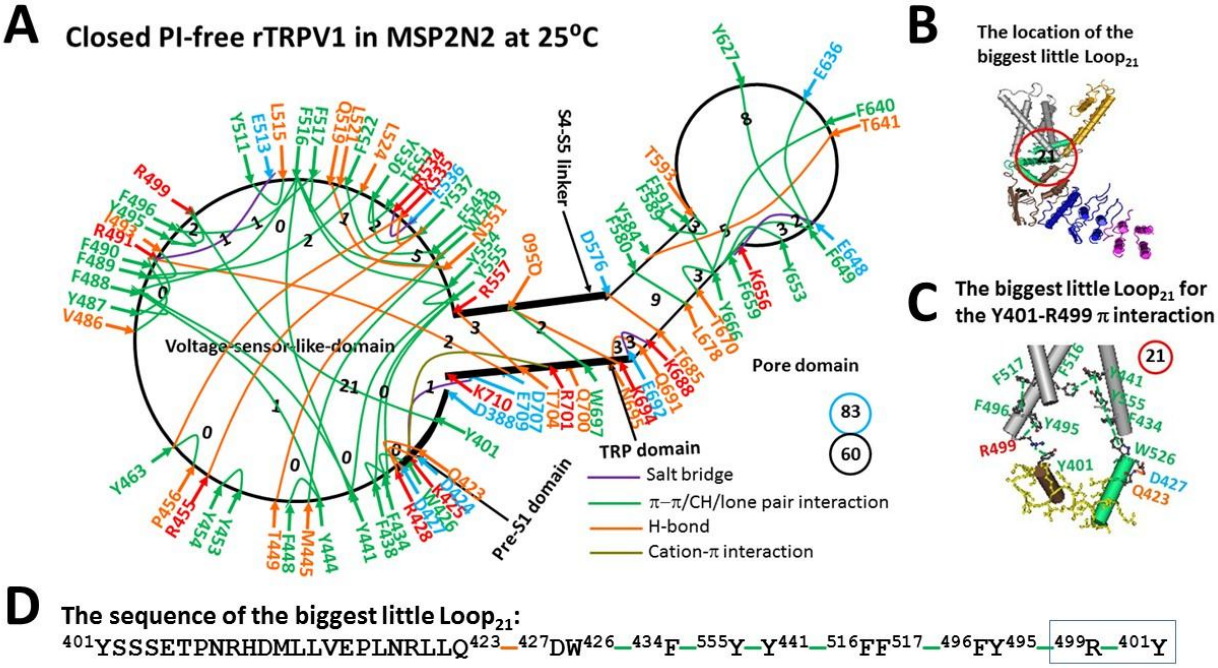

Figure 1

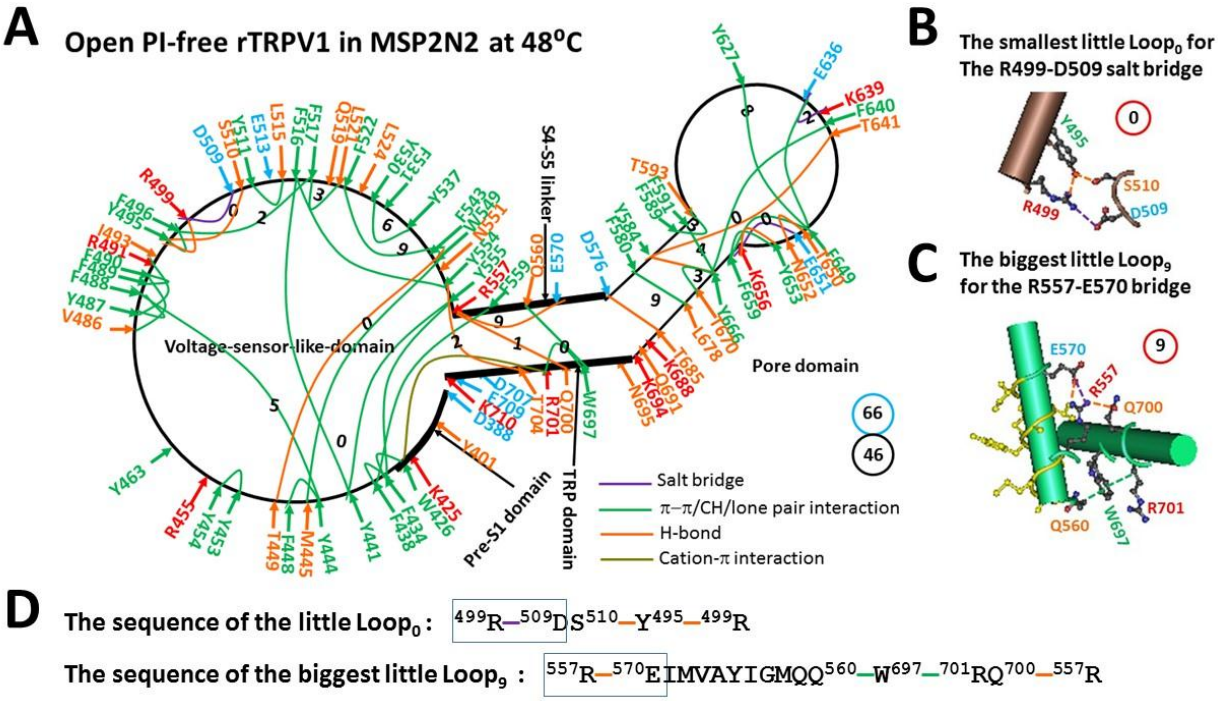

Figure 2

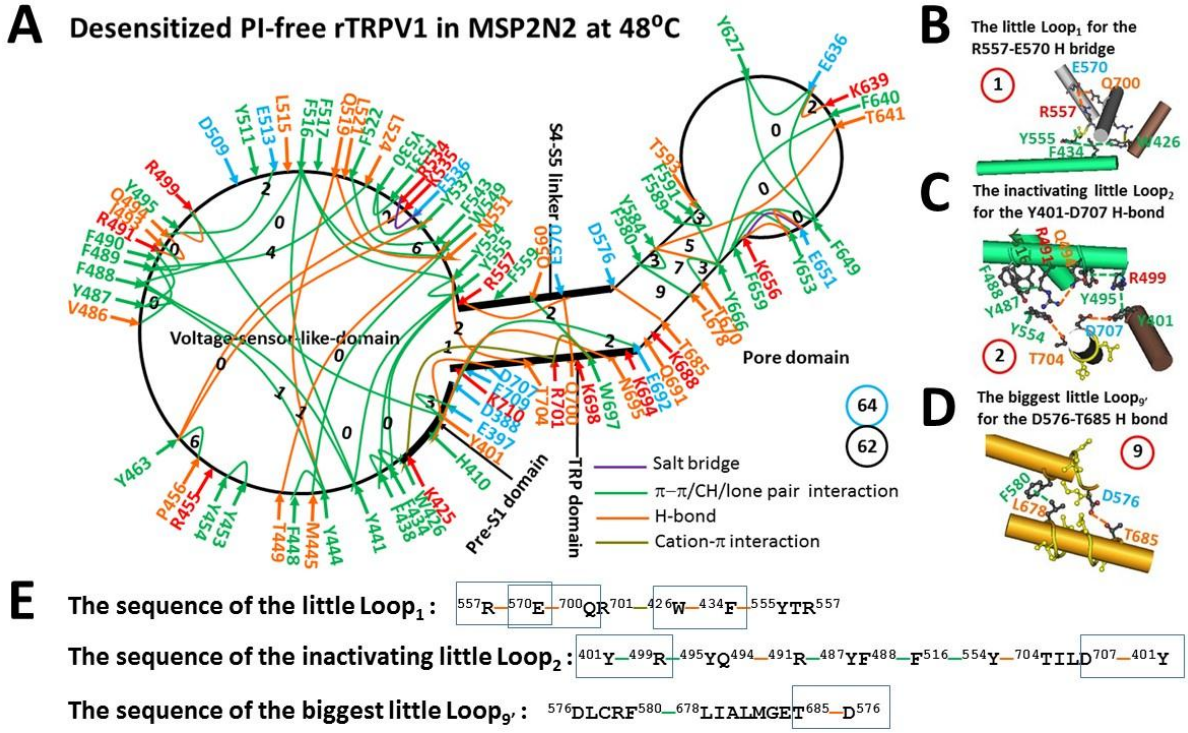

Figure 3

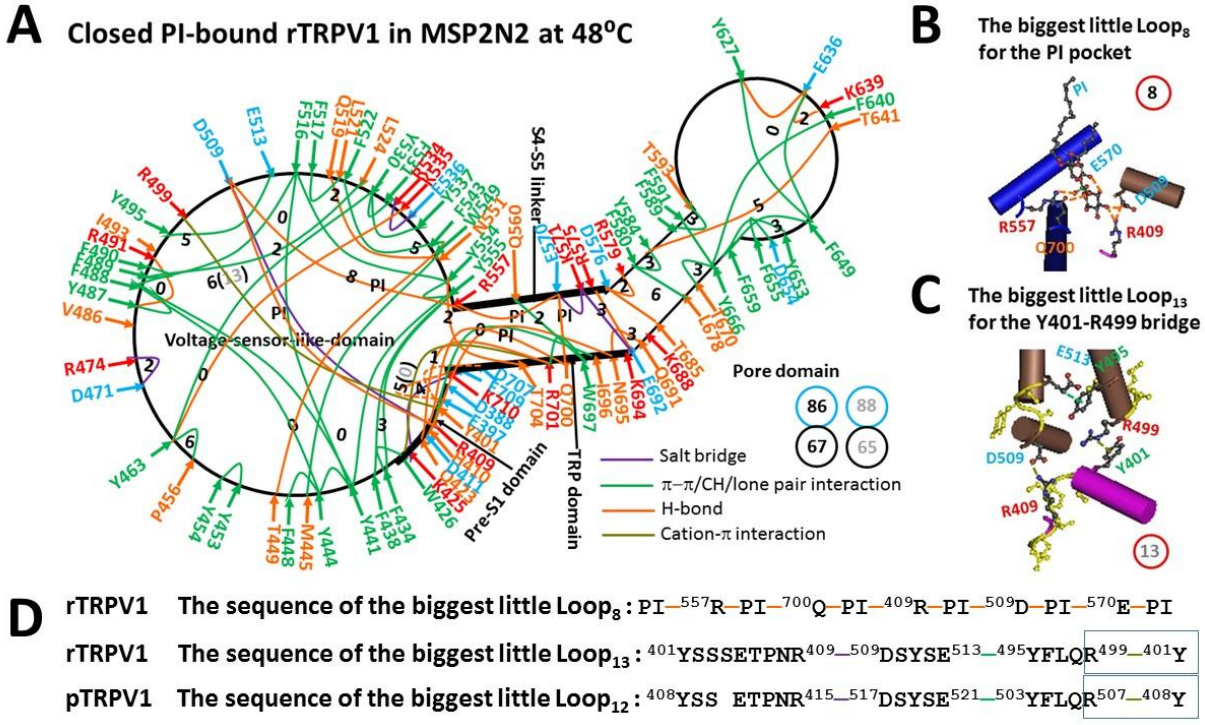

Figure 4

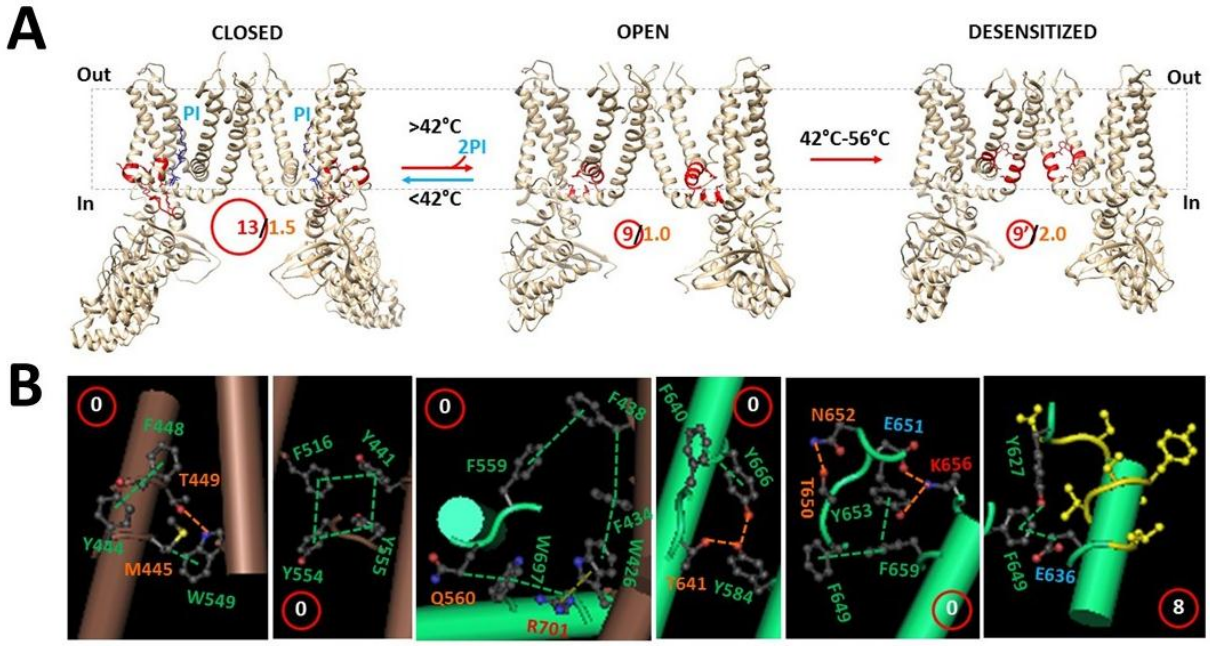
A
CLOSED
OPEN
DESENSITIZED
Out
In
PI
PI
>42°C
2PI
<42°C
42°C-56°C
13/1.5
9/1.0
9/2.0
B
F448
T449
Y444
M445
W549
F516
Y441
Y554
Y555
F559
F438
W697
F436
W426
Q560
R701
F640
Y666
T641
Y584
N652
E651
K656
T650
Y653
F659
F649
Y627
F649
E636

Figure 5